SPIE Defense + Commercial
Geospatial Informatics X
Conf. 11398, Session 5: Environmental and Geospatial Analytics
Wednesday, April 29, 2020

SAND2020-4132C

Robust Terrain Classification of High-Spatial Resolution Remote Sensing Data Employing Probabilistic Feature Fusion and Pixelwise Voting

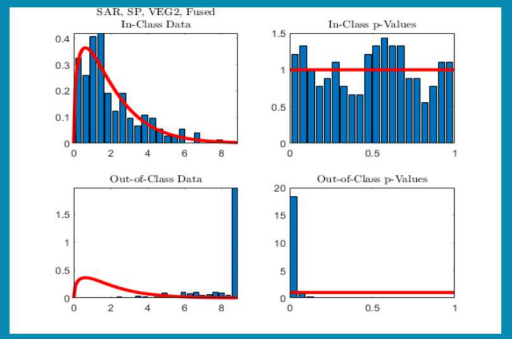

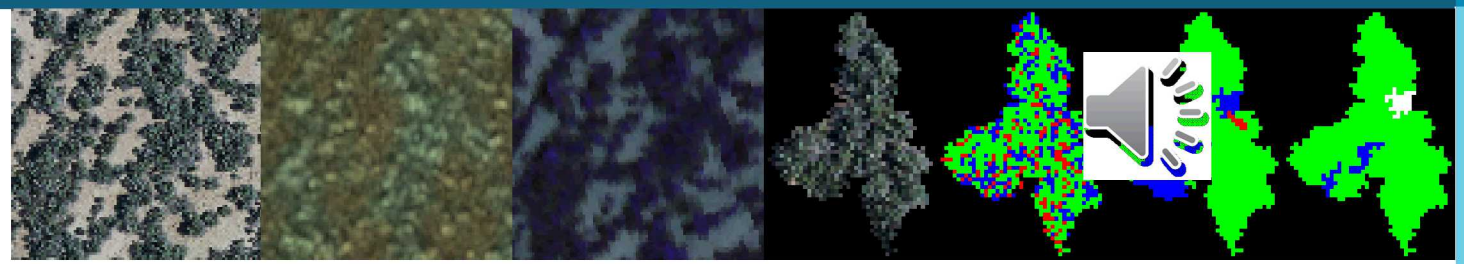

PRESENTED BY

David A. Yocky, **R. Derek West**, Brian J. Redman,
John D. van der Laan, and Dylan Z. Anderson

dayocky@sandia.gov, rdwest@sandia.gov

Sandia National Laboratories is a multimission laboratory managed and operated by National Technology & Engineering Solutions of Sandia, LLC, a wholly owned subsidiary of Honeywell International Inc., for the U.S. Department of Energy's National Nuclear Security Administration under contract DE-NA0003525.
SAND2020-XXXX C

Hypothesis

High-spatial resolution remote sensing images contain a high degree of in-class variability within terrain classes.

Techniques robust to high variability, such as ensemble voting, can improve the performance of terrain classification in high-resolution remote sensing data.

Transparent classifiers aide in the understanding of terrain classification.

Outline

- Remote Sensing Modalities
  - Optical Imagery
  - Hyper-Spectral Imagery (HSI)
  - Polarimetric Synthetic Aperture Radar (PolSAR)
- Terrain Classification Framework
  - Terrain Classes
  - Pixels vs. Superpixels
  - Probabilistic Feature Fusion
  - Pixelwise Voting
- Performance Metrics
- Questions

Remote Sensing Modalities

Optical Images

- Collected with a commercial DSLR camera
  - Standard Bayer RGB filter
  - Integrated with the onboard navigation system
  - 0.025 m pixel spacing
  - cted June, 2016
- Feature vector, class specific transformation:

$$\boldsymbol{v}_{RGB} = [R \quad G \quad B]^T$$

$$\boldsymbol{v}_{OPT,CLS} = \Gamma^{CLS}\boldsymbol{v}_{RGB}$$

Hyperspectral Images (HSI)

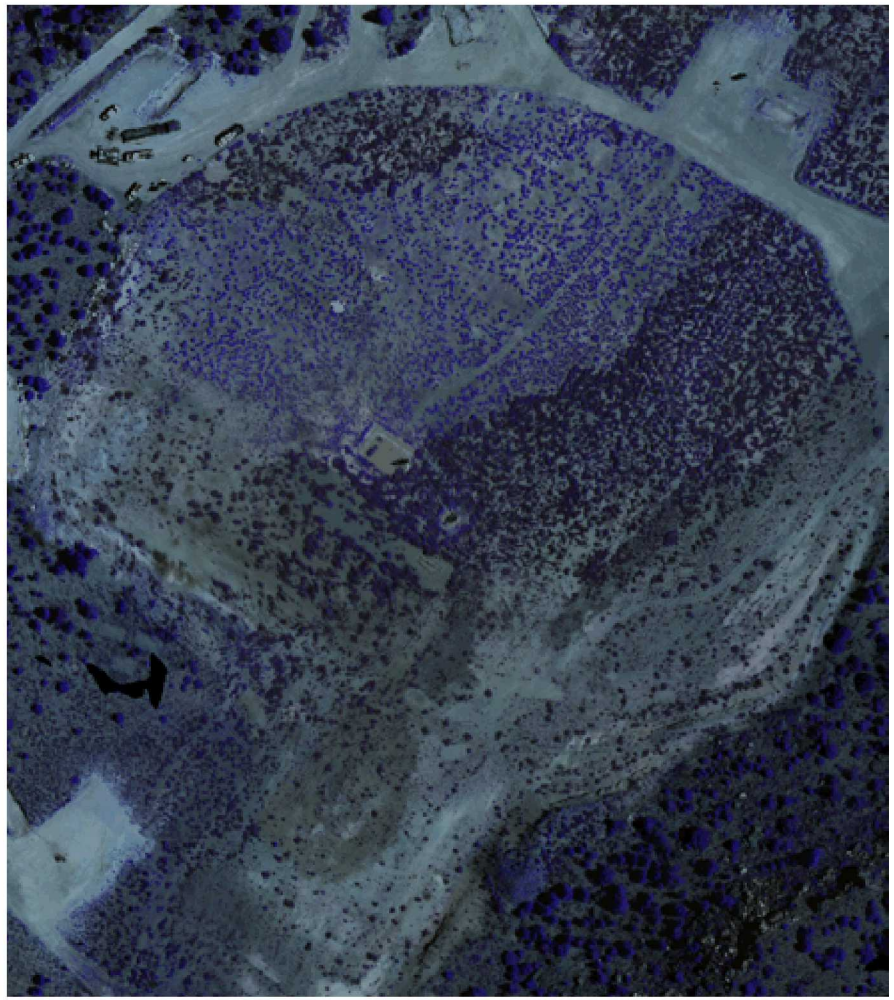

- Collected with a linear pushbroom VNIR sensor
  - Over 270 bands, $\lambda \approx 400 - 1000$ nm
  - Integrated with the onboard navigation system
  - 0.10 m pixel spacing
  - Collected June, 2016

- F e vector:

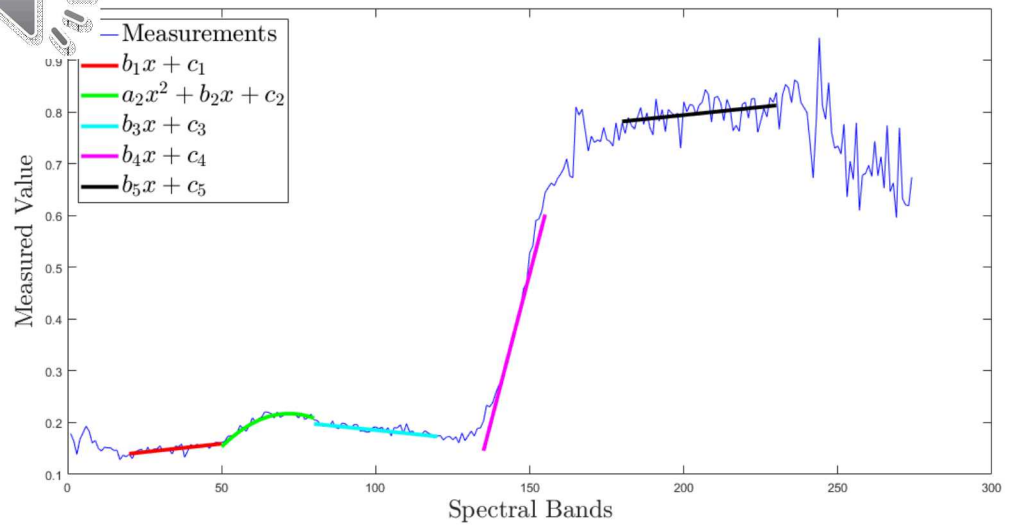

$$\boldsymbol{v}_{HSI} = [b_1 \quad c_1 \quad a_2 \quad b_2 \quad c_2 \quad b_3 \quad c_3 \quad b_4 \quad c_4 \quad b_5 \quad c_5]^T$$

Polarimetric Synthetic Aperture Radar (PolSAR) Images

- Collected with Sandia FARAD X-band radar
  - Fully-polarimetric VideoSAR
  - $R = 3460$ m, $\psi = 38°$
  - $\rho_r = 0.2032$ m, $\rho_a = 0.1563$ m
  - Multi-looked to reduce speckle
  - Collected March, 2016
- Feature vector contains:
  - Polarimetric decomposition parameters
    - H/A/α
    - G4U
  - Total power
  - Coherence (from two-passes)

$$\boldsymbol{v}_{SAR} = [H \quad \alpha \quad P_s \quad P_d \quad P_v \quad P_c \quad \zeta \quad \gamma]^T$$

Terrain Classification Framework

Terrain Classes

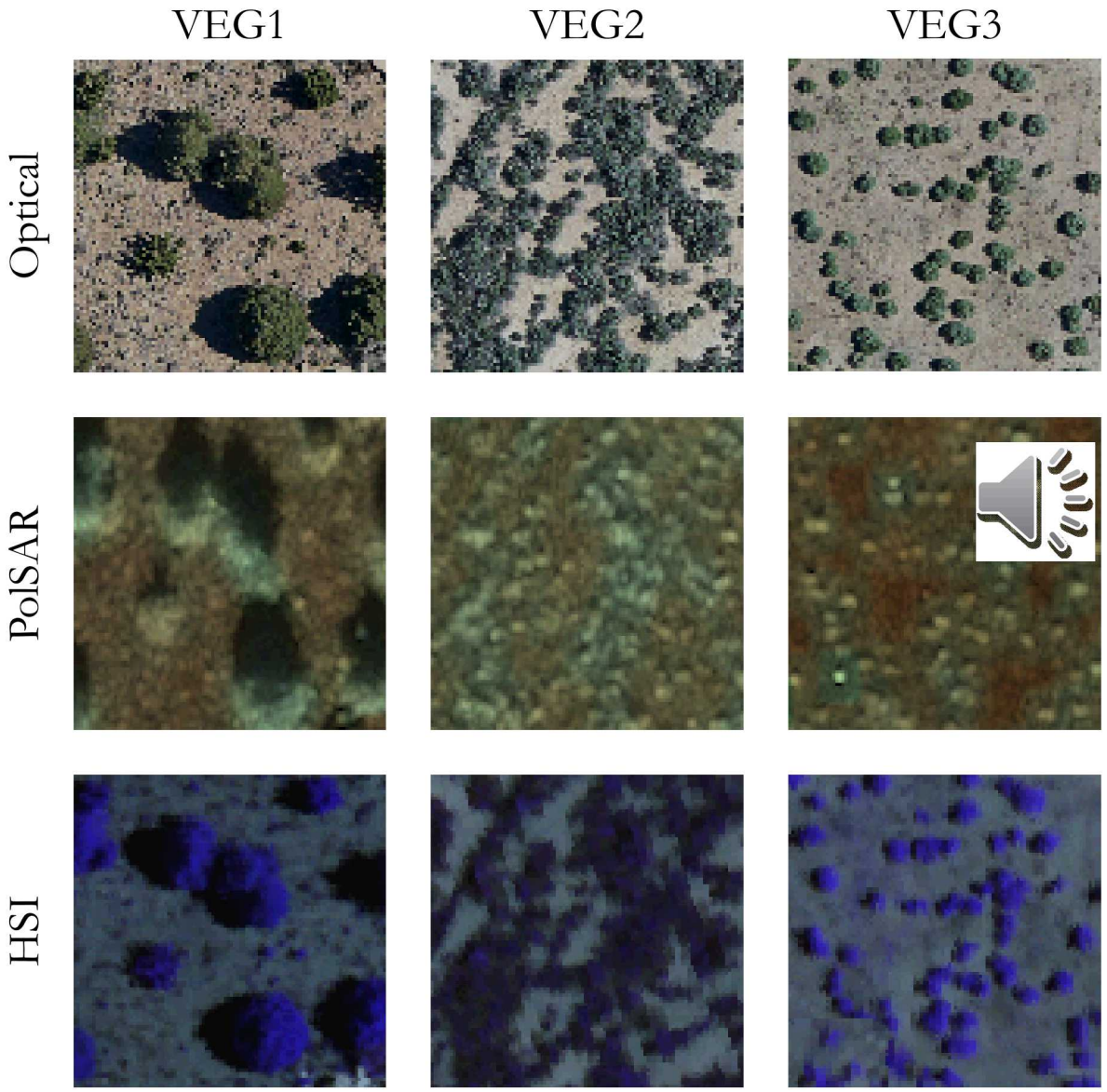

- Three vegetation classes
  - One tree class
  - Two low-vegetation classes
- Optical and HSI effectively have the same imaging geometry
- PolSAR images contain layover due to the imaging geometry (noticeable in the trees)

Pixels vs. Superpixels

High resolution Optical Image

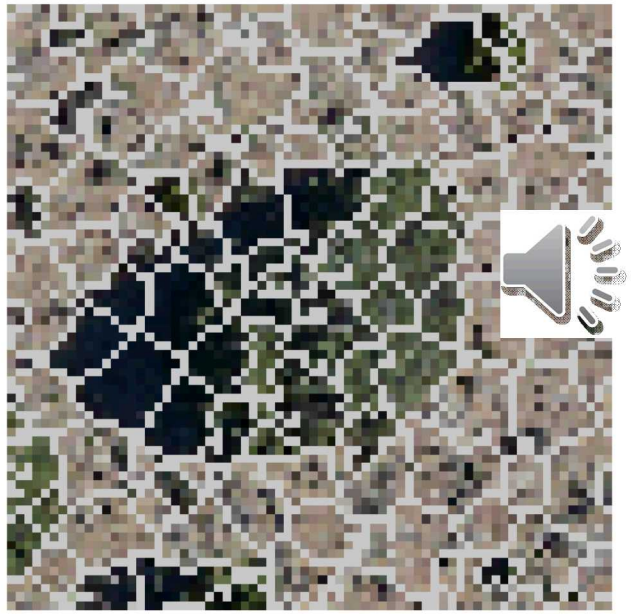

SLIC Superpixel Segmentation

- Terrain classes in high resolution imagery have higher pixel-to-pixel variability
  - Objects are composed of more pixels
  - Increased distribution spread of measured values
- There are methods to deal with increased class variability, such as a moving average
- SLIC superpixel segmentation algorithm
  - Set to produce nominally 40 pixels/superpixel
  - Excellent job delimiting contrasting boundaries
  - Statistics can be computed from the pixel values within a superpixel

Probabilistic Feature Fusion (PFF)

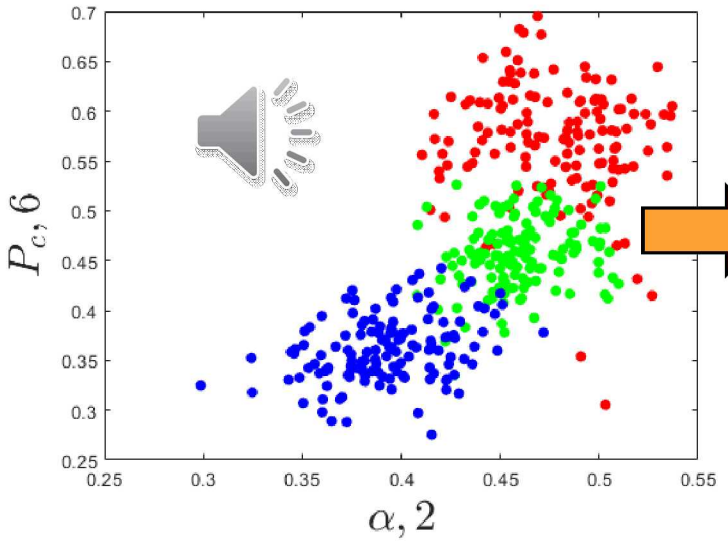

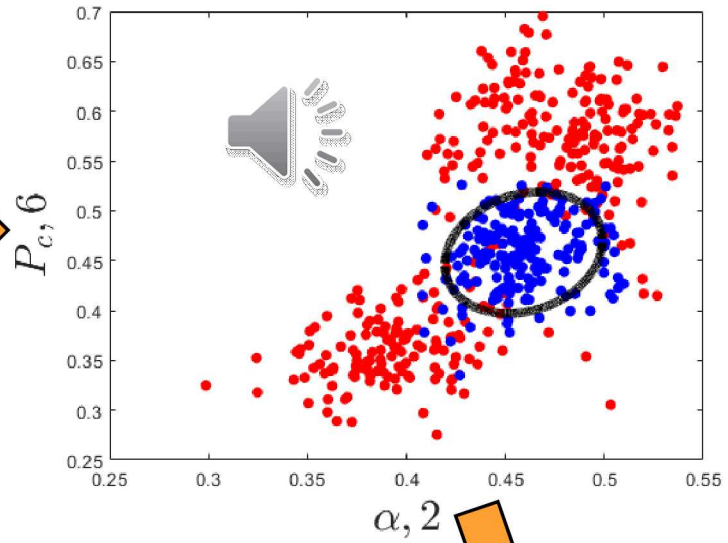

Class separation is noticeable in pairwise scatterplots of the feature vector data.

Only in-class data are modeled with PFF. PFF generates p-values that give a measure of in-class consistency with the training data.

The Mahalanobis distance was used for the HSI and PolSAR data.

The absolute distance from the mean was used for the optical data.

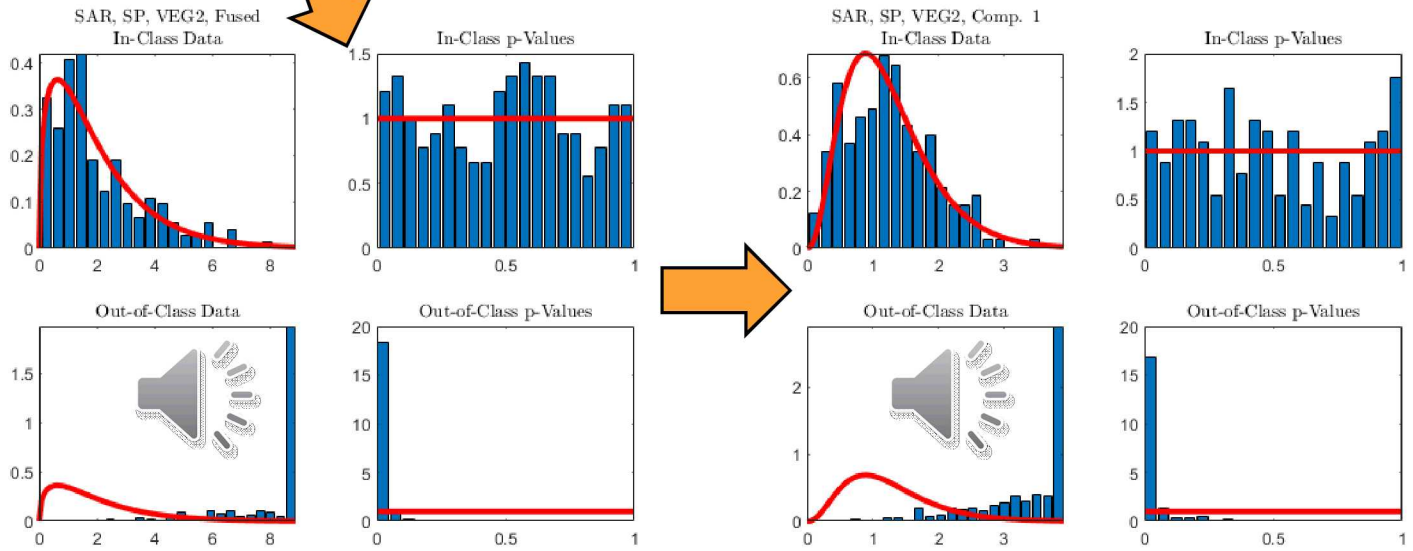

P-value Maps

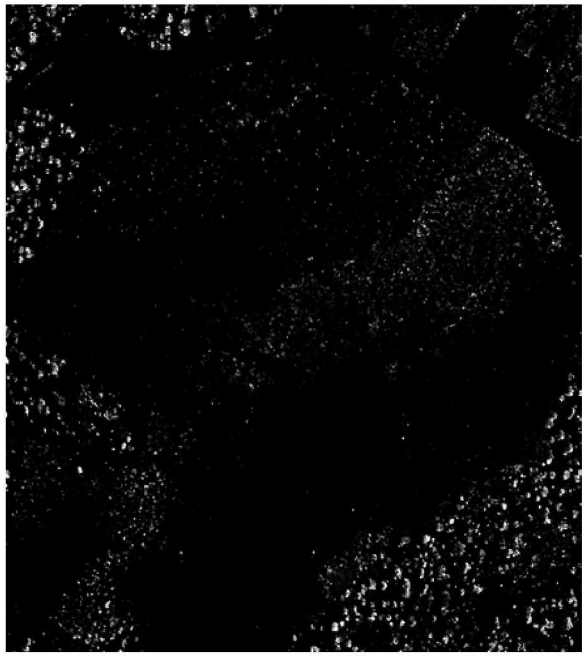

Feature 1

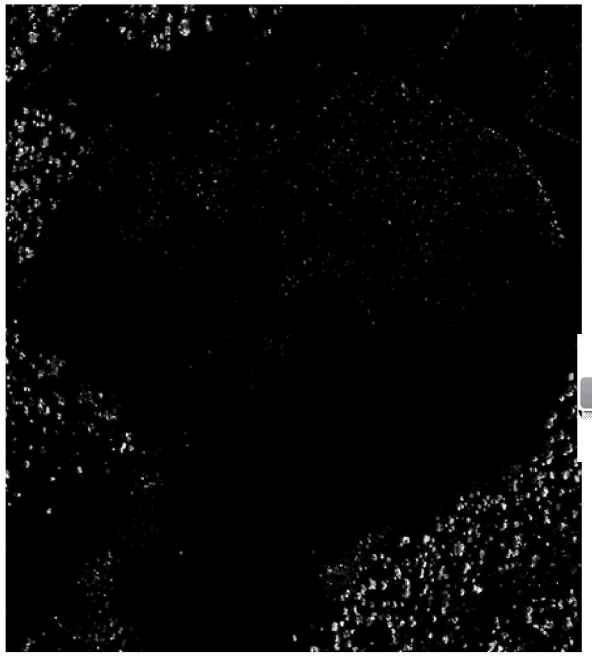

Feature 2

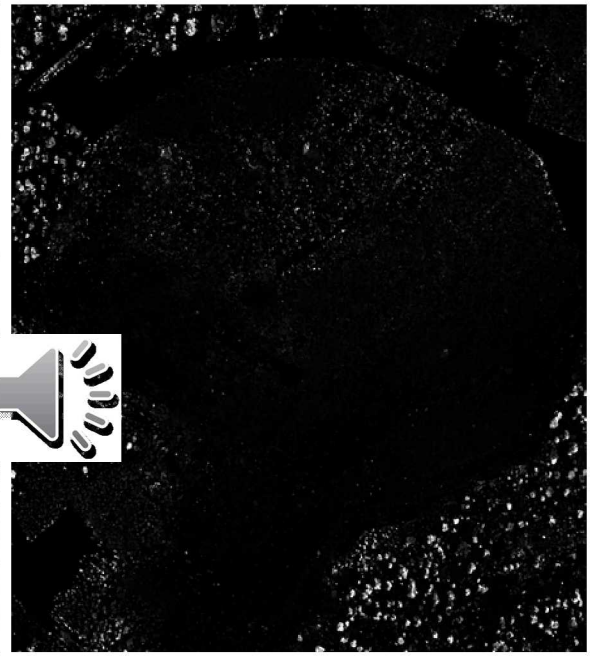

Feature 3

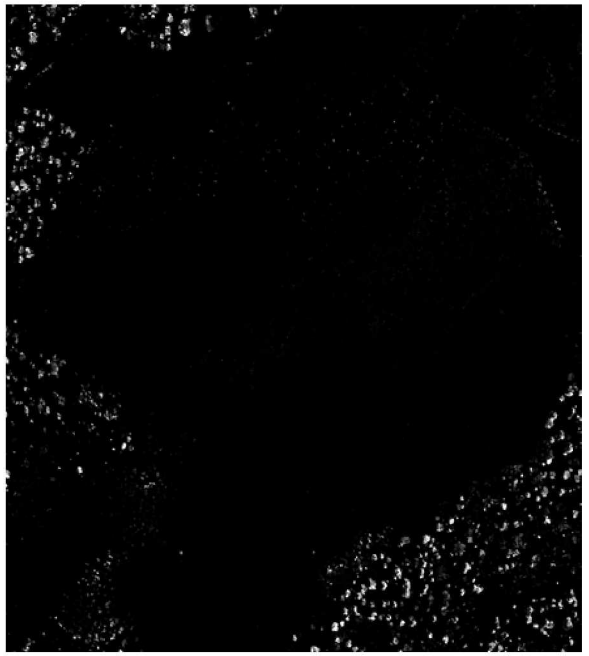

Fused

The p-value maps for the superpixel PFF model for VEG1 show good isolation from each feature.

The fused p-value map shows that the selected features have reduced potential for false alarms.

Pixelwise Voting

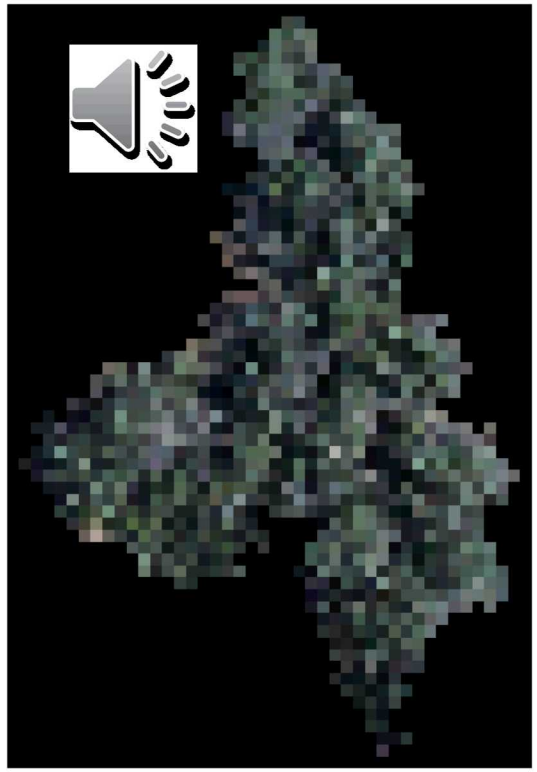

Region of VEG2

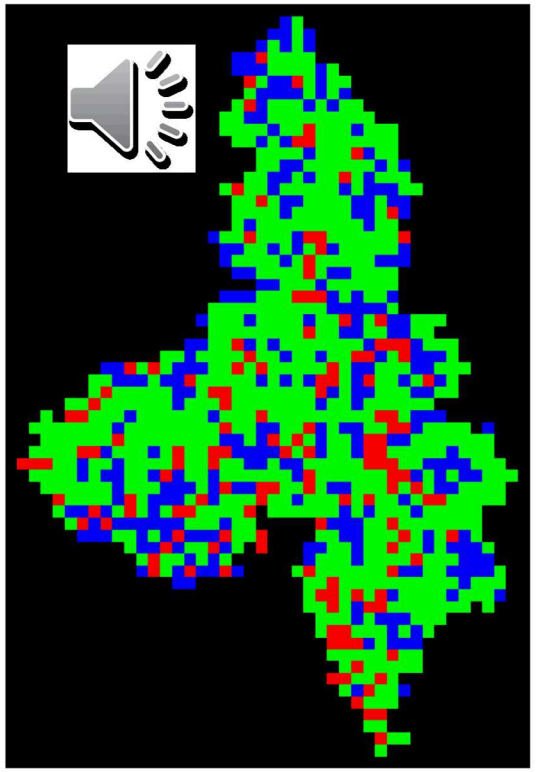

Pixelwise PFF Model

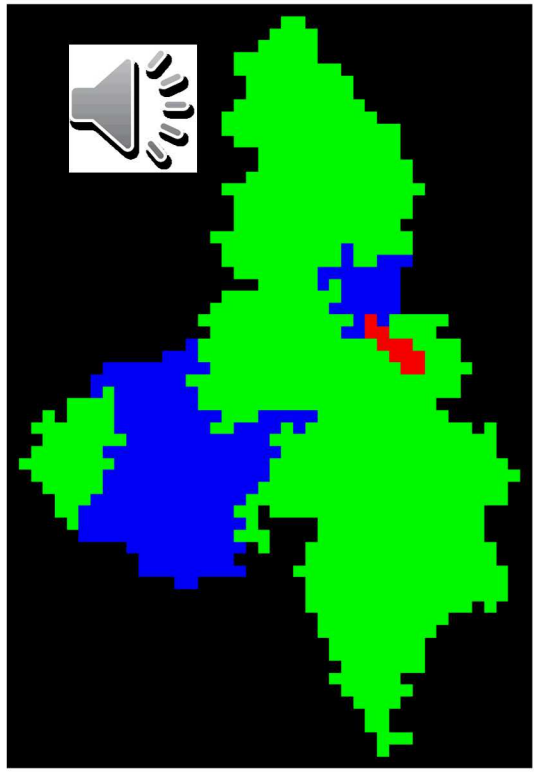

Superpixel PFF Model

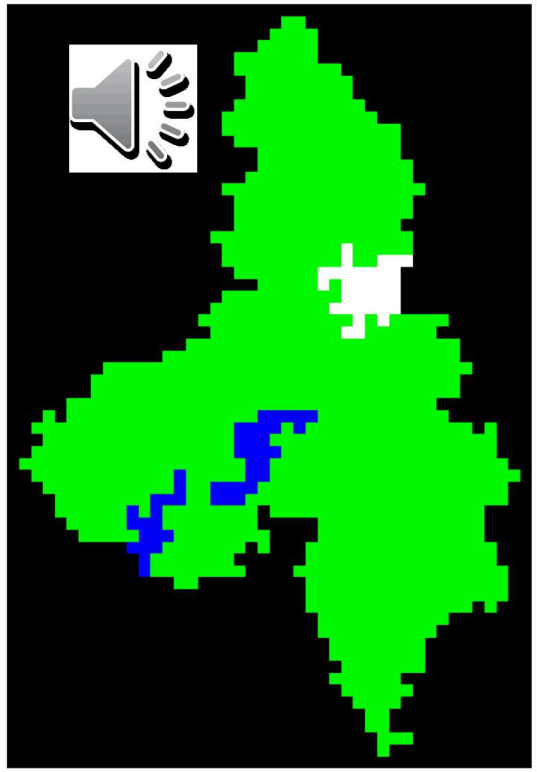

Pixelwise Voting

Pixelwise voting within a superpixel tends to increase the correct in-class declarations over pixelwise and superpixel methods.

Performance Metrics

Receiver Operating Characteristic (ROC) Curves

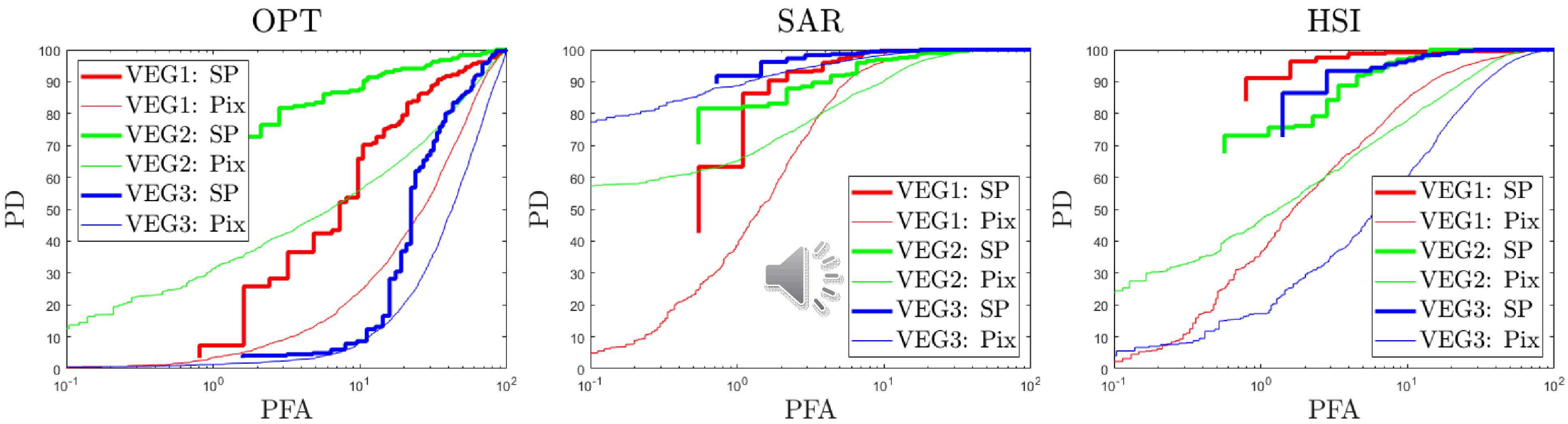

ROC curves show increased performance, higher percent detection (PD) with lower percent false alarms (PFA), operating at the superpixel level, as compared to the pixelwise level.

Optical Confusion Matrices

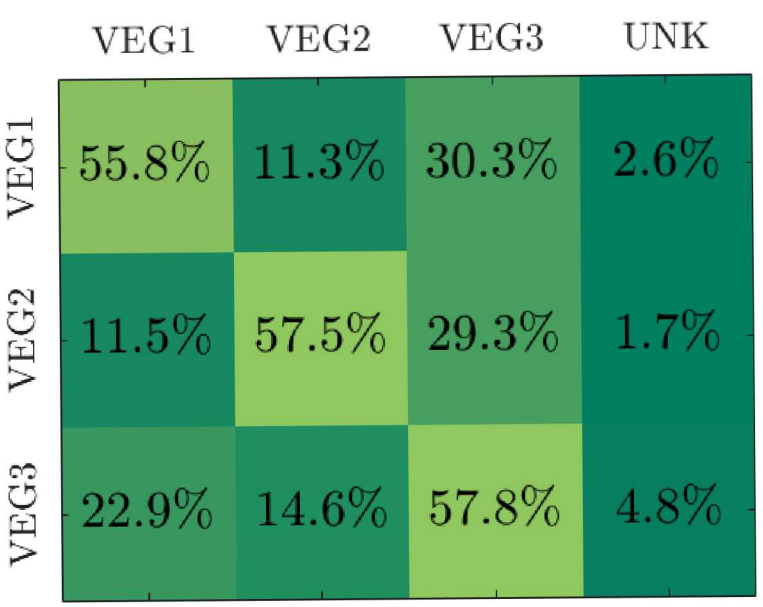

Pixelwise

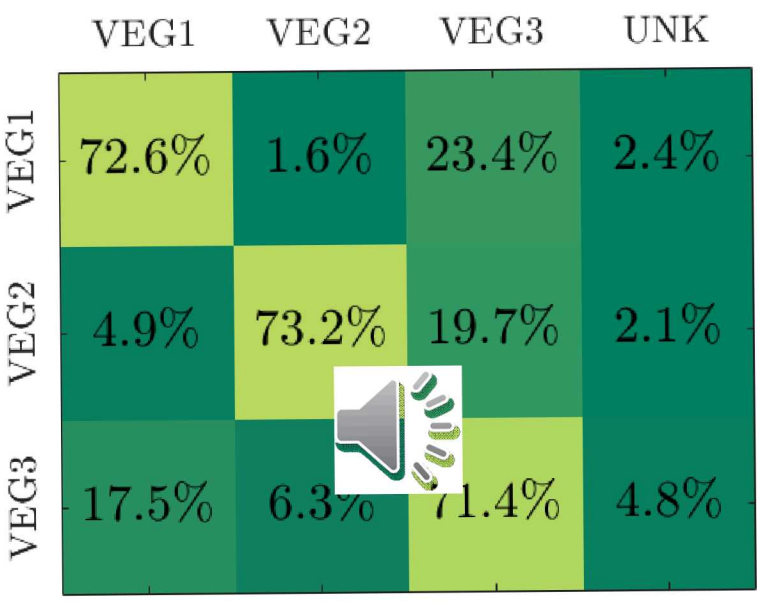

Superpixel

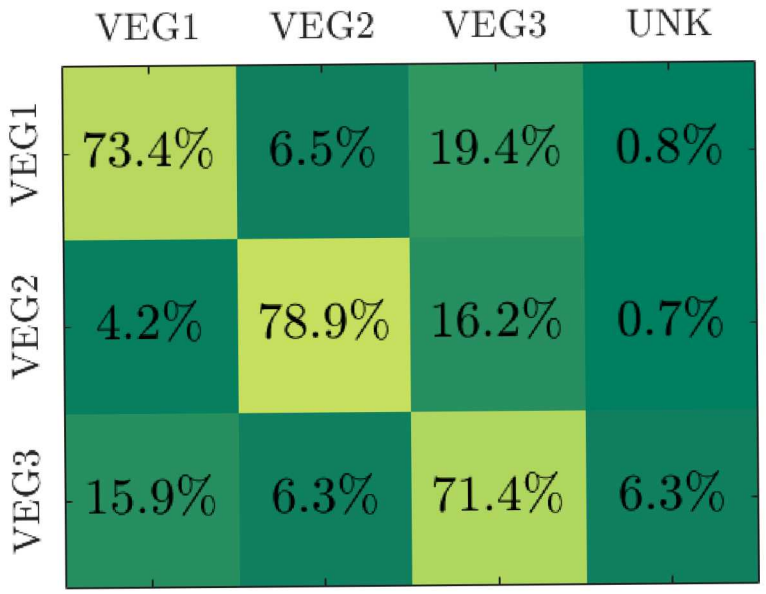

Pixelwise Voting

The in-class declarations increase from pixelwise, to superpixel, to pixelwise voting, with the exception of VEG3, where the superpixel and voting methods tie.

PolSAR Confusion Matrices

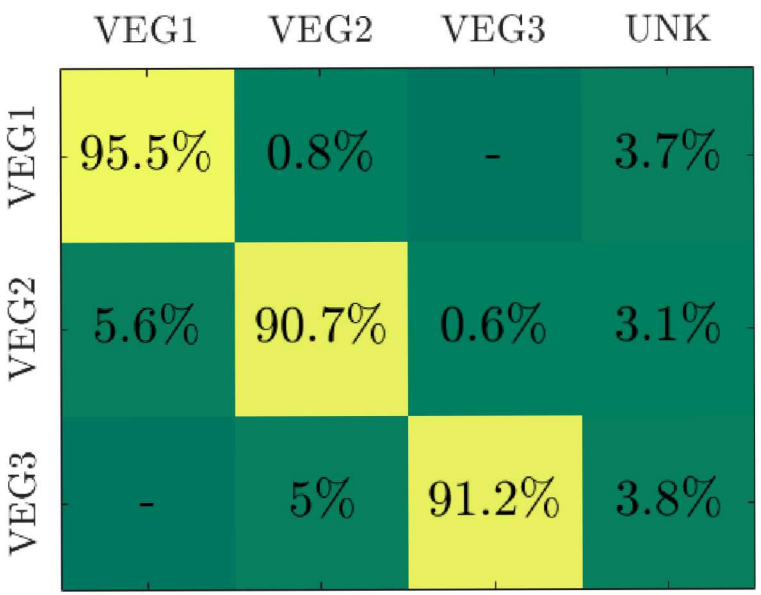

Pixelwise

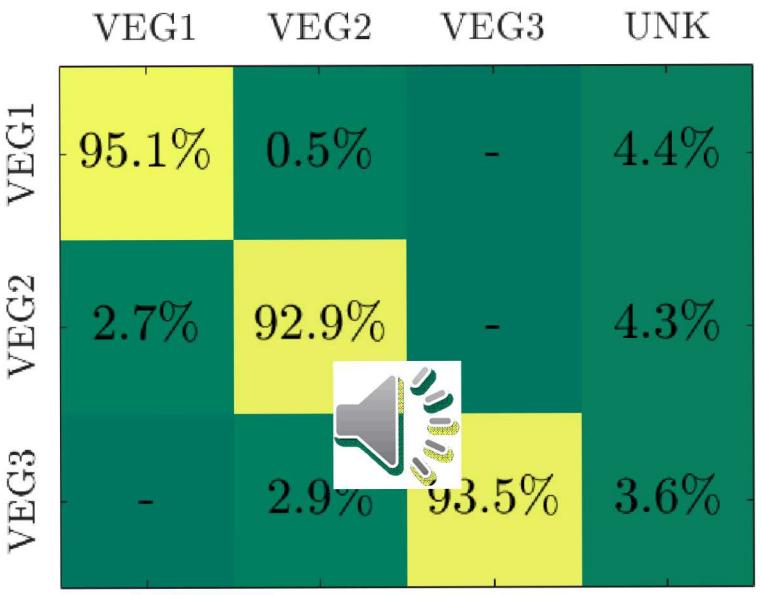

Superpixel

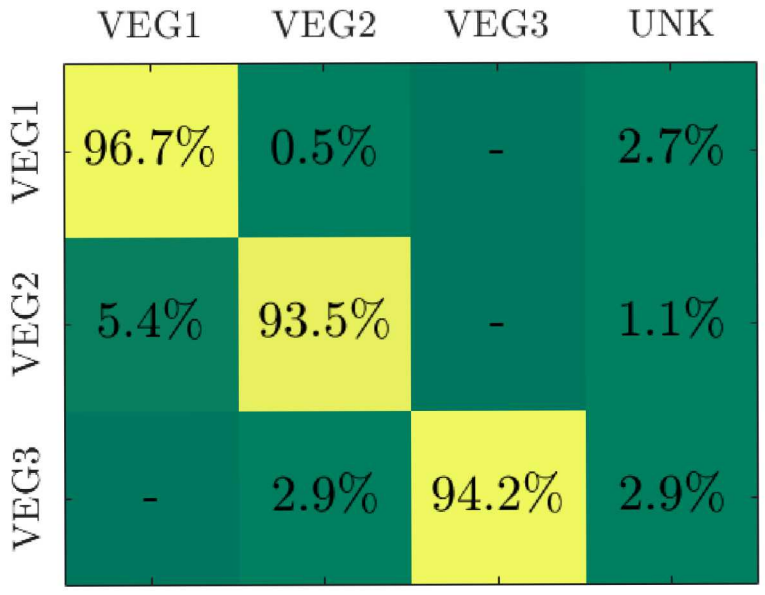

Pixelwise Voting

The pixelwise voting method has the best in-class performance on the PolSAR data.

HSI Confusion Matrices

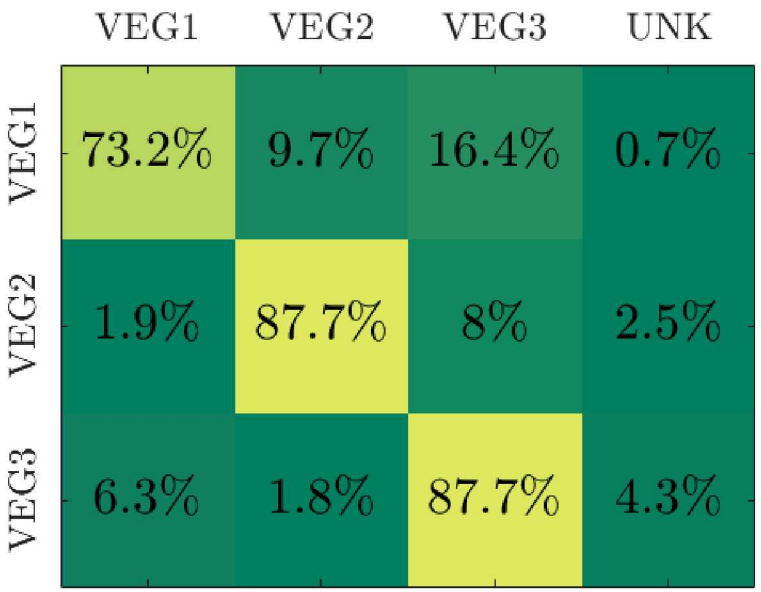

Pixelwise

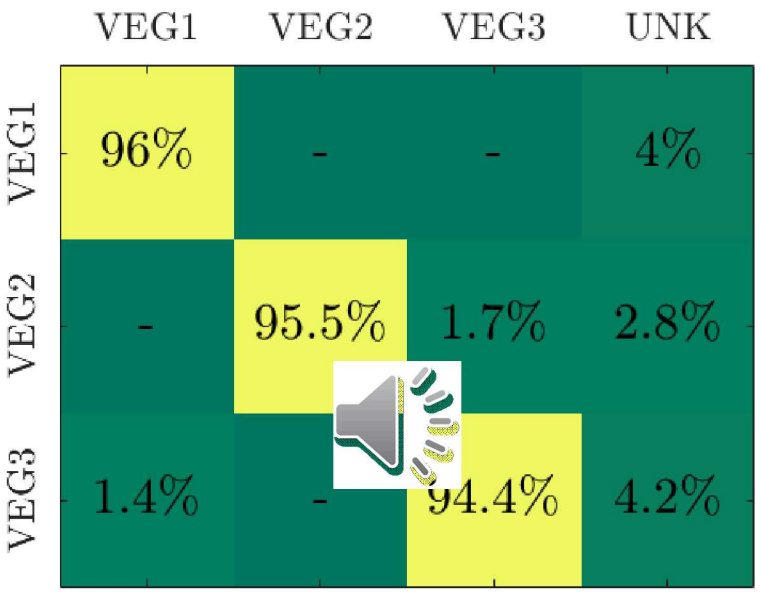

Superpixel

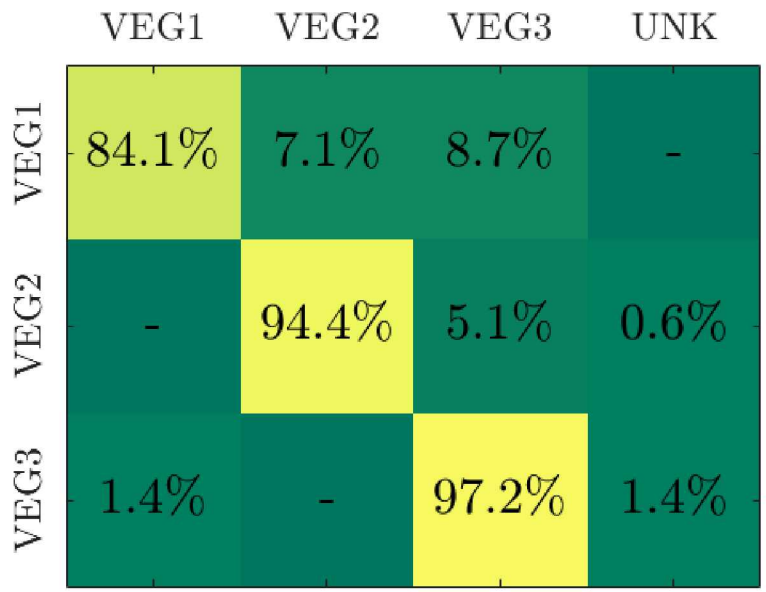

Pixelwise Voting

The pixelwise voting method only has the best in-class performance in one class of the HSI data. The superpixel method has the best performance in the other two classes.

Classifiers Applied to Optical Image

Pixelwise

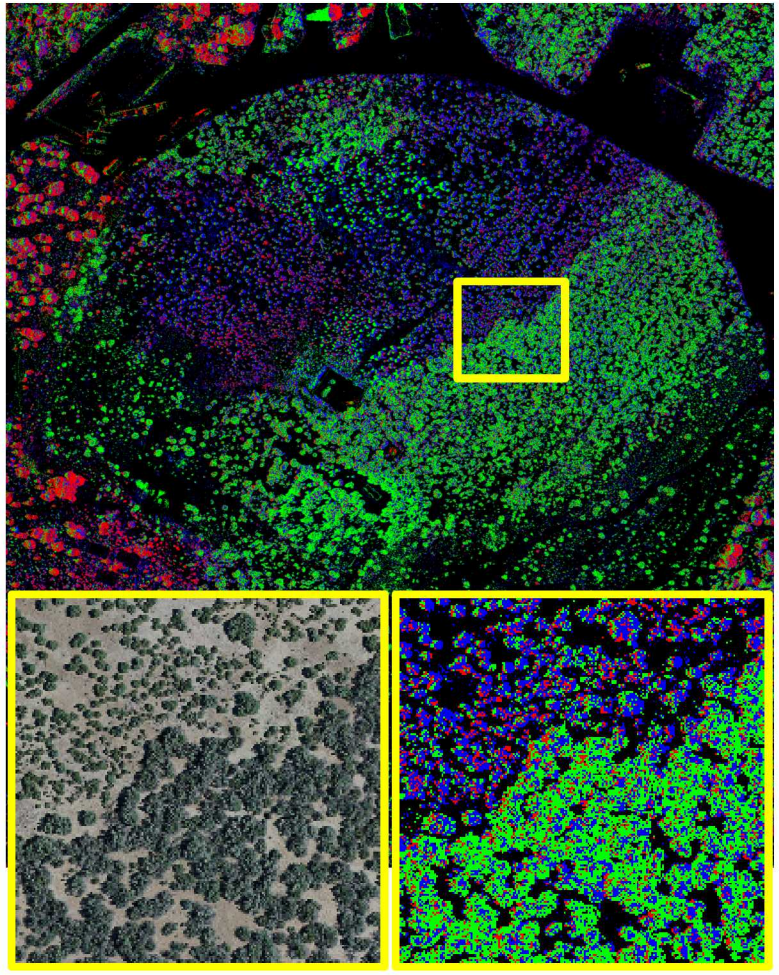

Superpixel

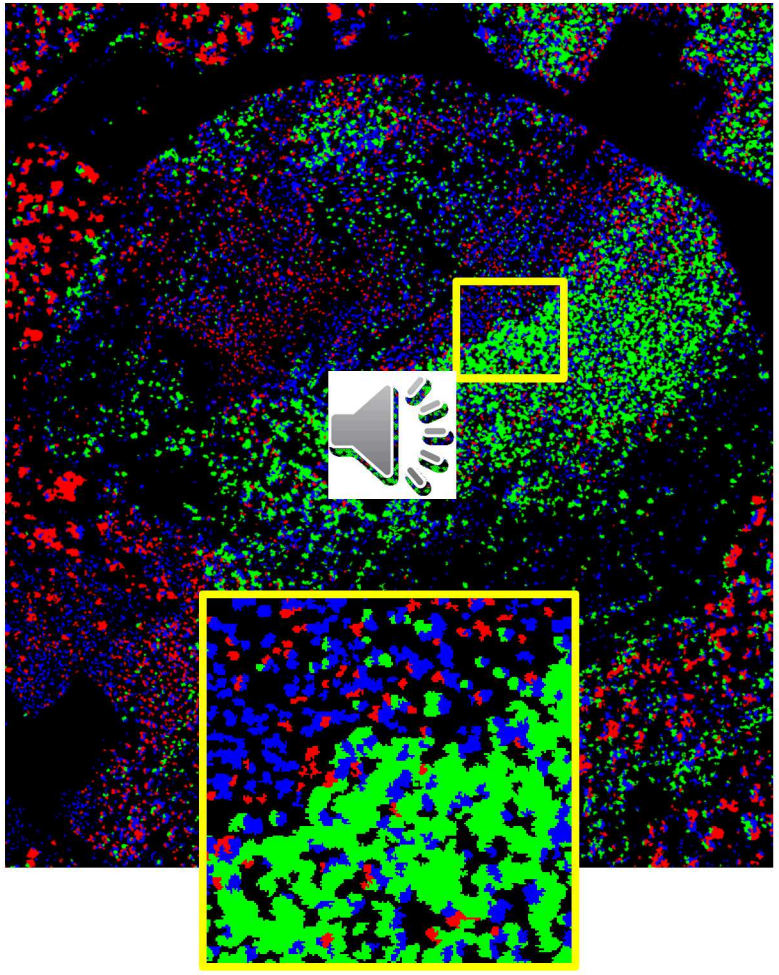

Pixelwise Voting

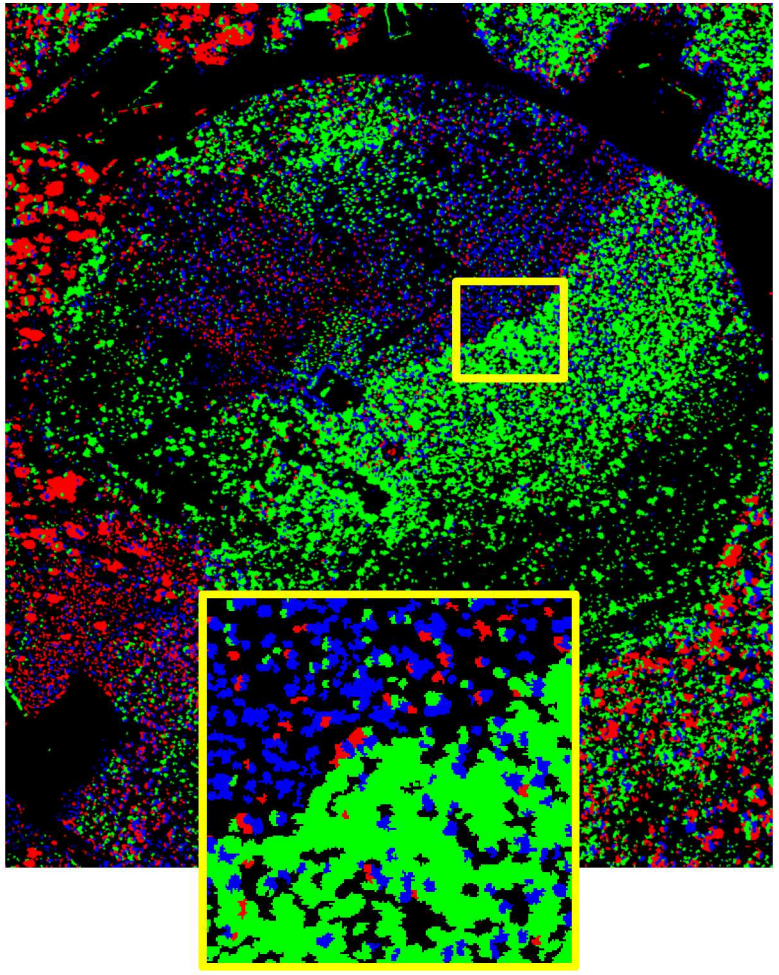

In general, both the superpixel and voting methods have less spatial variability in the declared classes, as compared to the pixelwise output; however, there are still many mis-classifications. The p-value threshold was set to 0.10.

Classifiers Applied to PolSAR Image

Pixelwise

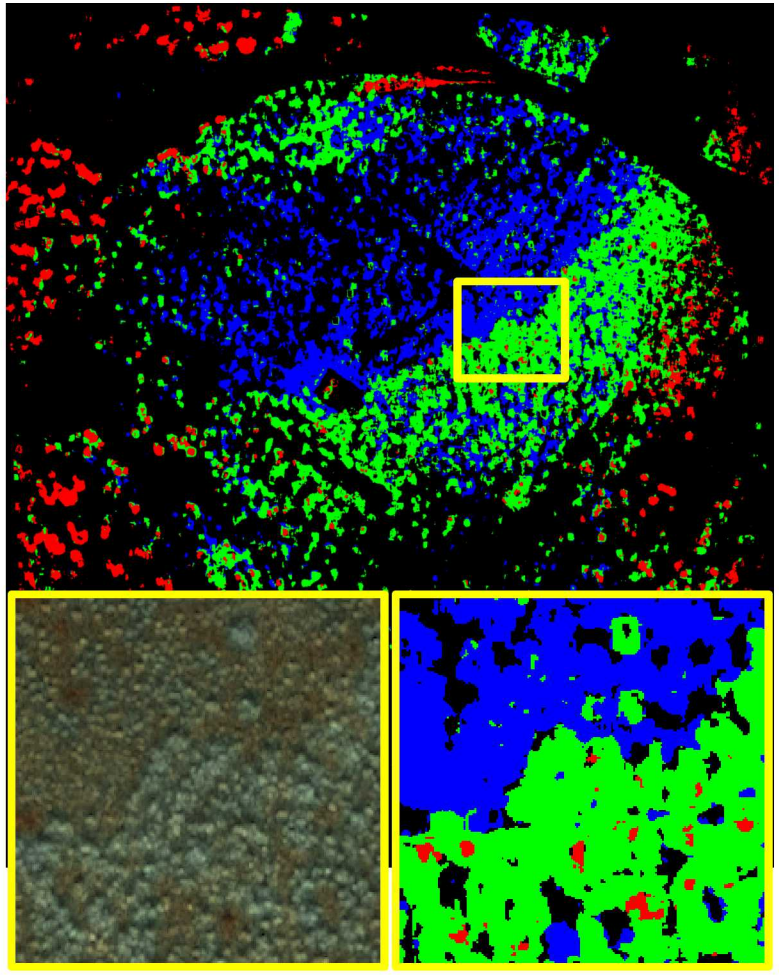

Superpixel

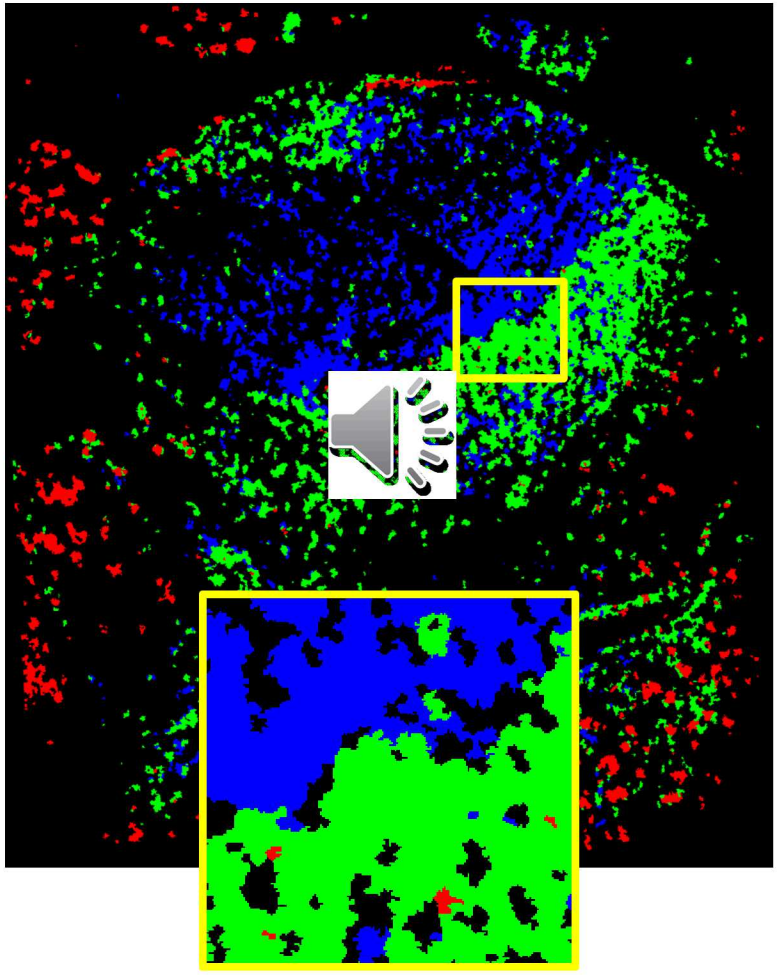

Pixelwise Voting

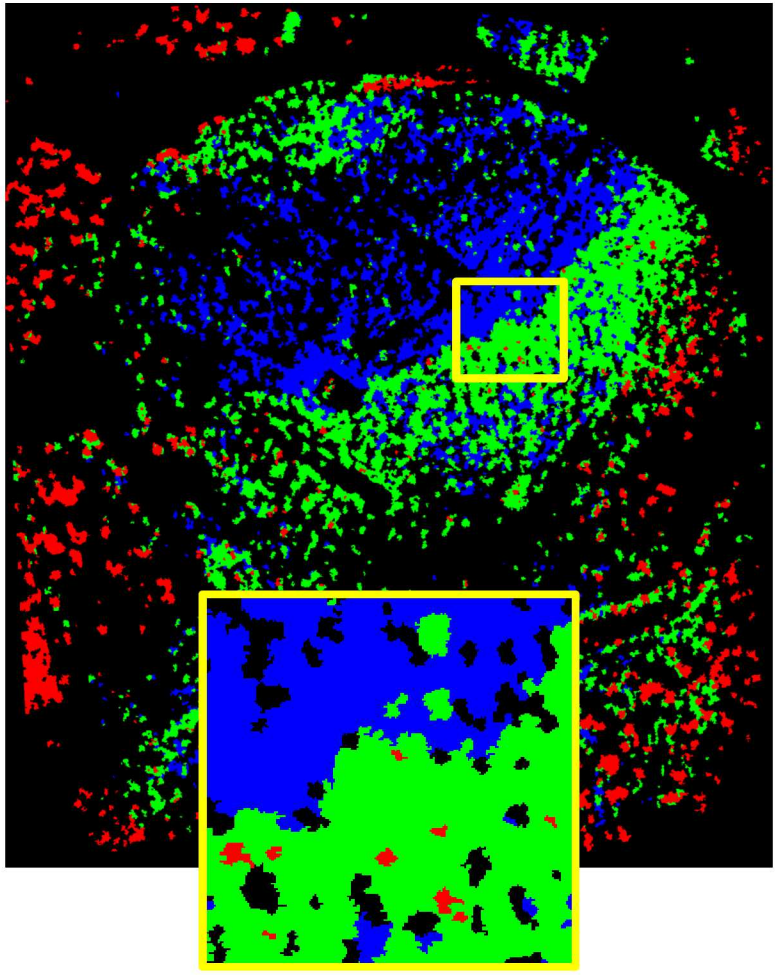

The superpixel and voting methods again have the least spatial variability in the declared classes; however, there are still a few mis-classifications. The p-value threshold was set to 0.10.

Classifiers Applied to Hyperspectral Image

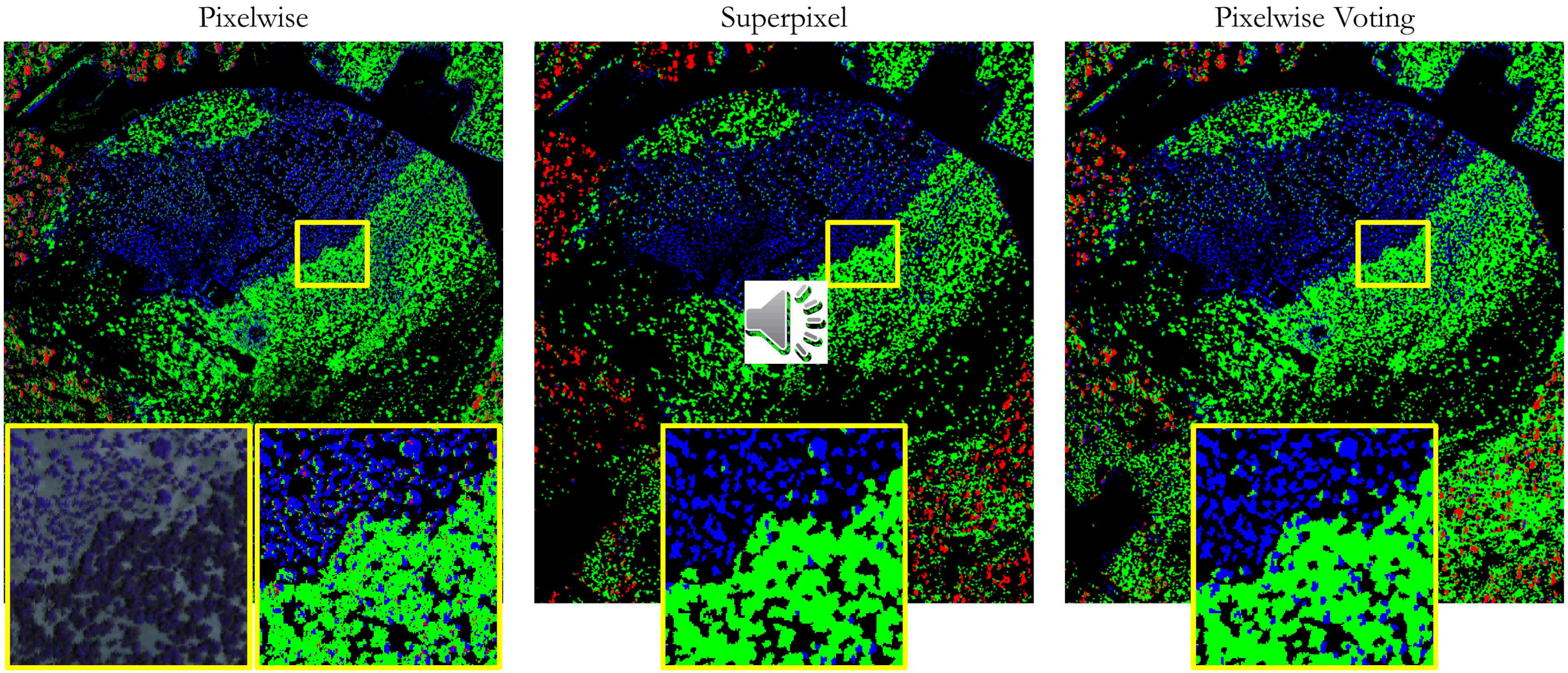

The superpixel and voting methods have less spatial variability in the declared classes; however, there are still a few mis-classifications. The p-value threshold was set to 0.10.

Conclusion

- Terrain classes have more pixelwise variability in high resolution imagery
  - Pixelwise classifiers are prone to have more mis-classifications
  - Terrain typically does not need high resolution
- We introduced a framework for making more robust terrain decisions
  - Segment images into superpixels to delimit contrasting regions
  - Train probabilistic feature fusion pixelwise classifie[illegible]ach terrain class
  - Make terrain decisions at the superpixel level by sel[illegible]g the majority vote
- Preliminary performance metrics indicate that this methodology tends to work well
  - Optical and PolSAR benefitted the most
  - HSI showed an improvement over pixelwise decisions, but superpixel decisions did well, too
- Application of the voting decision method shows drastically less spatial variability than pixelwise decisions and is not quite as conservative as the superpixel decisions.

Questions?

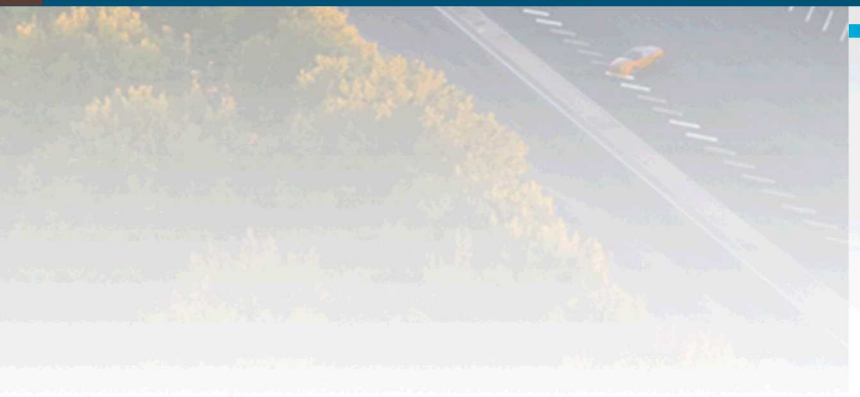

References

Jong-Sen Lee, Grunes, M. R., Pottier, E., and Ferro-Famil, L., "Unsupervised terrain classification preserving polarimetric scattering characteristics," IEEE Transactions on Geoscience and Remote Sensing 42, 722-731 (April 2004).

Vandapel, N., Huber, D. F., Kapuria, A., and Hebert, M., "Natural terrain classification using 3-d ladar data," in IEEE International Conference on Robotics and Automation, 2004. Proceedings. ICRA '04. 2004, 5, 5117-5122 (April 2004).

Lalonde, J.-F., Vandapel, N., Huber, D. F., and Hebert, M., "Natural terrain classification using three-dimensional ladar data for ground robot mobility," Journal of Field Robotics 3(10), 839-861 (2006).

West, R. D., LaBruyere III, T. E., Skryzalin, J., Simonson, K. M., Hansen, R. L., and Van Benthem, M. H., "Polarimetric SAR Image Terrain Classification," IEEE Journal of Selected Topics in Applied Earth Observations and Remote Sensing 12, 4467-4485 (Nov 2019).

Chia-Tang Chen, Kun-Shan Chen, and Jong-Sen Lee, "The use of fully polarimetric information for the fuzzy neural classification of SAR images," IEEE Transactions on Geoscience and Remote Sensing 41, 2089-2100 (Sep. 2003).

Bau, T. C., Sarkar, S., and Healey, G., "Hyperspectral region classification using a three-dimensional gabor filterbank," IEEE Transactions on Geoscience and Remote Sensing 48, 3457-3464 (Sep. 2010).

Kuang, D. and Xu, J., "Combined multiple spectral-spatial features and multikernel support tensor machine for hyperspectral image classification," Journal of Applied Remote Sensing 14(3), 1-16 (2019).

Anderson, D., Craven, J. M., Dzur, R., Briggs, T., Lee, D. J., Miller, E., Schultz-Fellenz, E., and Vigil, S., "Using unmanned aerial systems to collect hyperspectral imagery and digital elevation models at a legacy underground nuclear test site," in SPIE Conference on Image Sensing Technologies: Material, Devices, Systems, and Applications V, 10656, UNSP 1065605 (Apr 2018).

Simonson, K. M., West, R. D., Hansen, R. L., LaBruyere, T. E., and Van Benthem, M. H., "A statistical approach to combining multisource information in one-class classifiers," Statistical Analysis and Data Mining: The ASA Data Science Journal 10(4), 199-210 (2017).

NOAA, N., "OPUS: Online positioning user service," (February 2018).

"OTB" Version 5.6.1."

Jakowatz, Jr., C. V., Wahl, D. E., Eichel, P. E., Ghiglia, D. C., and Thompson, P. A., Spotlight-mode Synthetic Aperture Radar: A Signal Processing Approach, Springer (1996).

Wahl, D. E., Eichel, P. H., Ghiglia, D. C., and Jakowatz, C. V., "Phase gradient autofocus-a robust tool for high resolution SAR phase correction," IEEE Transactions on Aerospace and Electronic Systems 30,827-835 (Jul 1994).

Cloude, S. R. and Pottier, E., "A review of target decomposition theorems in radar polarimetry," IEEE Transactions on Geoscience and Remote Sensing 34, 498-518 (Mar 1996).

Singh, G., Yamaguchi, Y., and Park, S. E., "General four-component scattering power decomposition with unitary transformation of coherency matrix," IEEE Transactions on Geoscience and Remote Sensing 51, 3014-3022 (May 2013).